1984

Atmospheric Environment Vol. 18, No. 8, pp. 1601–1611, 1984
Printed in Great Britain.

0004-6981/84 $3.00 + 0.00
Pergamon Press Ltd.

ESTIMATION OF LAGRANGIAN TIME SCALES FROM LABORATORY MEASUREMENTS OF LATERAL DISPERSION

WEN-WHAI LI and ROBERT N. MERONEY

Fluid Mechanics and Wind Engineering Program, Department of Civil Engineering, Colorado State University, Fort Collins, CO 80521, U.S.A.

(*First received 7 September* 1983; *in revised form* 4 *January* 1984 *and in final form* 17 *February* 1984)

Abstract—Field experiments and wind tunnel simulation results for the behavior of lateral plume dispersion are compared to three semi-emperical expressions based on the Taylor's diffusion theory. These relations imply a direct connection between dispersion coefficients and the Lagrangian integral time scale. The implied Lagrangian integral time scale was found to vary by as much as a factor of 15, depending on the relation used. Agreement between the field data and lateral measurements supports using wind tunnel results to simulate atmospheric transport.

1. INTRODUCTION

The distribution of atmospheric contaminates downwind from a continuous point source determines the relative environmental impact or hazard to the public. Reliable predictive relations applicable to a broad range of scales are not yet known. Indeed, most atmospheric transport predictive schemes for such a release still depend upon relations between mean wind field characteristics measured at a particular site and regression formulae developed from data collected at other sites at other times. Such parameterization requires a knowledge of vertical or horizontal growth of the plume or dominant characteristics of the turbulence field such as the Lagrangian autocorrelation function.

This paper examines the lateral dispersion characteristics of data from various field and laboratory experiments. These data are compared to alternative semi-emperical expressions which describe the growth of the plume lateral standard deviation with time. These expressions imply significantly different magnitudes for the Lagrangian integral time scales, which have been compared with time scale estimates proposed by four previous investigators. The similarity found between the laboratory data and field dispersion results supports the use of another alternative methodology for estimating atmospheric dispersion based on wind tunnel results and real time anemometer statistics.

2. REVIEW OF STATISTICAL DISPERSION CONCEPTS

Taylor (1921) argued that in a stationary homogeneous turbulent flow field the particle mean square displacement may be related to the velocity fluctuation by the following expression

$$[X_i^2] = 2[u_i^2] \int_0^T \int_0^t {}_iR_L(\tau)\,d\tau\,dt, \qquad (1)$$

where [ ] indicates an ensemble average of N fluid particles and $[u_i^2]$ is the variance of the ith component of velocity fluctuations. ${}_iR_L(\tau)$ is the Lagrangian autocorrelation of the velocity fluctuations in the ith direction; and T is the diffusion time. The relation may not be valid for the along wind direction in a uniform shear flow (Monin and Yaglom, 1975), but it holds for the transverse and vertical directions in a stationary homogeneous turbulence field. Since atmospheric turbulence is not normally vertically homogeneous, Taylor's theory is not satisfactory for $[X_3^2]$; but fortunately, horizontal homogeneity is usually present in the atmospheric boundary layer.

Pasquill (1971) suggested a more explicit relationship for the diffusion parameter derived from Taylor's equation. For lateral dispersion

$$[X_2^2]^{1/2} = [u_2^2]^{1/2} T f_1(T/{}_2T_L), \qquad (2)$$

where ${}_2T_L$ is the Lagrangian integral time scale and

$${}_2T_L = \int_0^\infty {}_2R_L(\tau)\,d\tau.$$

Draxler (1976) examined diffusion data from eleven field experiments including elevated and ground release sources over a range of stratification conditions. Since it is difficult to determine the true Lagrangian integral time scale from field diffusion experiments, he introduced another time scale T_i, which is proportional to ${}_2T_L$. Draxler first suggested that the lateral plume growth may be related to time, T/T_i, for all data by

$$f_1 = \frac{1}{1 + 1.0(T/T_i)^{0.6}},$$

where T_i is defined as the diffusion time required for f_1 to become equal to 0.5. In order to satisfy the theoretical limit for f_1 at large time and to provide a satisfactory fit to the data, he replaced the above

CEP83-84-WWL-RNM-3

equation by

$$f_1 = \frac{1}{1 + 0.9(T/T_i)^{0.5}}. \quad (3)$$

The corresponding Lagrangian autocorrelation function may be derived from Taylor's equation and Equation (3). This yields

$${}_2R_L(\tau) = \frac{1 - 1.125\sqrt{\tau/T_i}}{(1 + 0.9\sqrt{\tau/T_i})^4}, \quad (4)$$

but this expression for the autocorrelation function has an unrealistic infinite negative slope in the limit as $\tau \to 0$.

Phillips and Panofsky (1982) re-examined Draxler's ideas and concluded that (4) is inconsistent with the theory of the inertial subrange (see, Tennekes, 1979) according to which $R(\tau)$ varies at $1 - C\tau$ near $\tau = 0$, where C is a constant. They replaced (3) by another form

$$f_1(T/T_i) = 0.617\left[T/T_i - \frac{(T_i/T)^2}{5.25}\ln(1 + 5.25\,T/T_i)\right]^{1/2}. \quad (5)$$

which was derived from a simple form for ${}_2R_L(\tau)$,

$${}_2R_L(\tau) = \frac{1}{(1 + \tau/{}_2T_L)^2}. \quad (6)$$

An exponential Lagrangian autocorrelation function is also consistent with the assumptions of inertial subrange theory (Tennekes, 1979). In addition, the exponential form is consistent with the concept of a Markov process and is frequently preferred by analysts (Neumann, 1978). If

$${}_2R_L(\tau) = e^{-\tau/{}_2T_L} \quad (7)$$

one obtains

$$f_1(T/T_i) = 0.541\left[\frac{T_i}{T} - \frac{(T_i/T)^2}{6.83}(1 - e^{-6.83\,T/T_i})\right]^{1/2}. \quad (8)$$

DATA ACQUISITION FROM ATMOSPHERIC WIND TUNNELS

New measurements reported in this study were obtained in the Micrometeorological Wind Tunnel (MWT) at Colorado State University (CSU). The MWT is specifically designed to model significant turbulent characteristics of the atmospheric boundary layer. Through selection of proper combinations of wind tunnel length, surface roughness, ambient wind speed, temperature stratification and boundary layer augmentation devices, a range of atmospheric situations may be simulated (Cermak, 1982). Turbulence and dispersion measurements discussed in this paper were performed over a smooth floor. A fully developed turbulent boundary layer, 13 m downwind from the entrance section, was obtained. Augmentation devices at the entrance included 1.27 cm roughness entrance strips and a 3.8 cm × 7.6 cm sawtooth fence. One set of turbulent intensity measurements during neutral stratification was performed with an additional spire array at the entrance. A more detailed description of the wind tunnel facility was prepared by Plate and Cermak (1963).

3.1. *Source configurations and concentration measurements*

In earlier measurements a neutrally buoyant, continuous point source was tagged by Krypton-85 (Chaudhry and Meroney, 1973) or by a methane or ethane mixture (Li and Meroney, 1982). Dispersion from ground source releases was examined by Chaudhry and Meroney during neutral, stable and slightly stable stratifications.

New measurements were performed downwind of eight different source heights during neutral and stable stratification. Forty-five crosswind samples were taken at nine different downwind distances for each release height. Hydrocarbon tracers were evaluated by a Hewlett-Packard flame ionization detector Series 5700 Chromatograph. Samples were held in 50 hypodermic syringes until evaluation.

3.2. *Boundary layer flow characteristics*

Turbulent intensities were measured by utilizing a multiple-hotwire probe and anemometer. The probe incorporated a conventional cross wire and a low current resistence temperature wire. The cross wire was sensitive to both velocity and temperature fluctuations, whereas the temperature wire sensed only temperature fluctuations. Signals were recorded simultaneously and processed by a Hewlett-Packard 1000 computer.

In addition to the general turbulence statistics measurements, longitudinal Eulerian space–time correlations were measured at eight different heights in the neutrally stratified boundary layer. Velocity correlation measurements were performed for the same wind tunnel flow configuration as the dispersion measurements. Part of the experimental results will be presented in a later section; however additional results from these measurements will be published in the near future. Laboratory details may be found in the preliminary report by Li and Meroney (1982).

The flow parameters for different dispersion simulations are listed in Table 1. Figure 1 presents the lateral turbulent intensity in the simulated boundary layers whose stratification is characterized by various Richardson numbers, $Ri_\delta = (g/T)/(\Delta T\delta/U_\infty^2)$, where δ is the boundary layer thickness and U_∞ is the free stream velocity. Lateral turbulent intensities were consistent with earlier measurement by Arya (1969) as shown in Fig. 2. A lateral intensity of turbulence $\sqrt{u_2'^2}/U_\infty = 0.02$ was selected for the analysis of dispersion during stable stratification. Similarly, from Fig. 3, $\sqrt{u_2'^2}/U_\infty = 0.04$ was adopted for the analysis of dispersion during neutral stratification.

Table 1. Summary of experimental conditions

Run	Source position	Thermal stratification	U_∞ (cm s^{-1})	ΔT (°F)	δ (cm)	u_* (cm s^{-1})	Ri_δ	z_0 (cm)
NG*	Ground	Neutral	300	0	73	12.40	0	2.44×10^{-3}
SG 1*	Ground	Stable	300	80	70	17.70	0.104	2.44×10^{-3}
SG 2*	Ground	Stable	600	80	72	7.34	0.0234	2.44×10^{-3}
NP	Ground Elevated	Neutral	200	0	45	7.76	0	2.20×10^{-3}
SP	Ground Elevated	Stable	200	82	70	10.93	0.25	6.95×10^{-2}

* From Chaudhry and Meroney (1973).

δ = boundary layer thickness, u_* = friction velocity, Ri_δ = reference Richardson number and z_0 = roughness length.

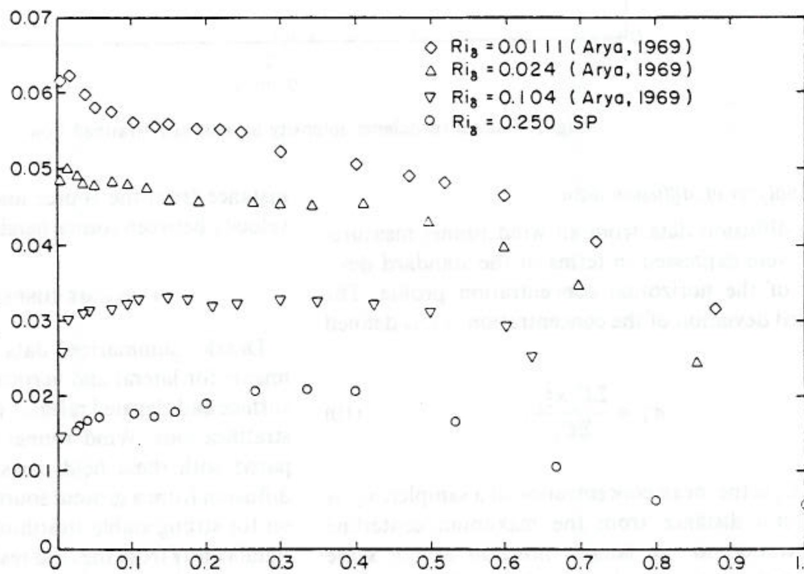

Fig. 1. Lateral turbulence intensity under stable stratification.

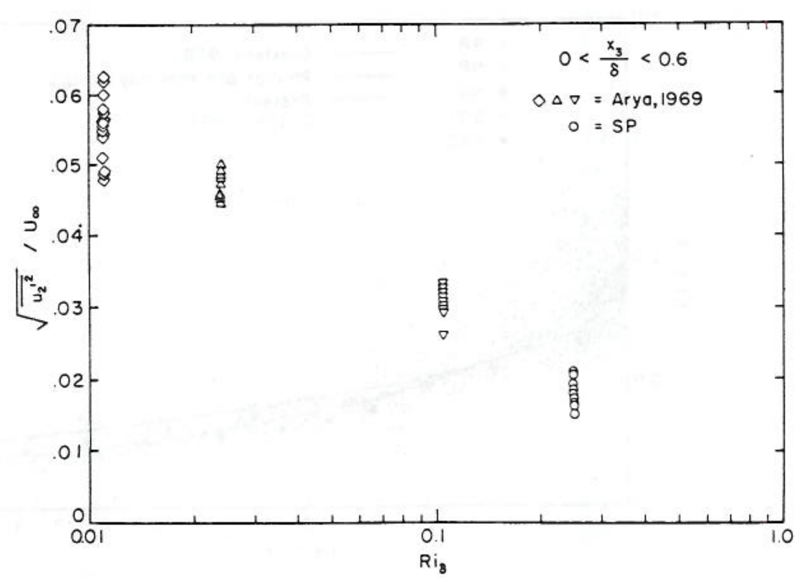

Fig. 2. Lateral turbulence intensity vs Richardson number.

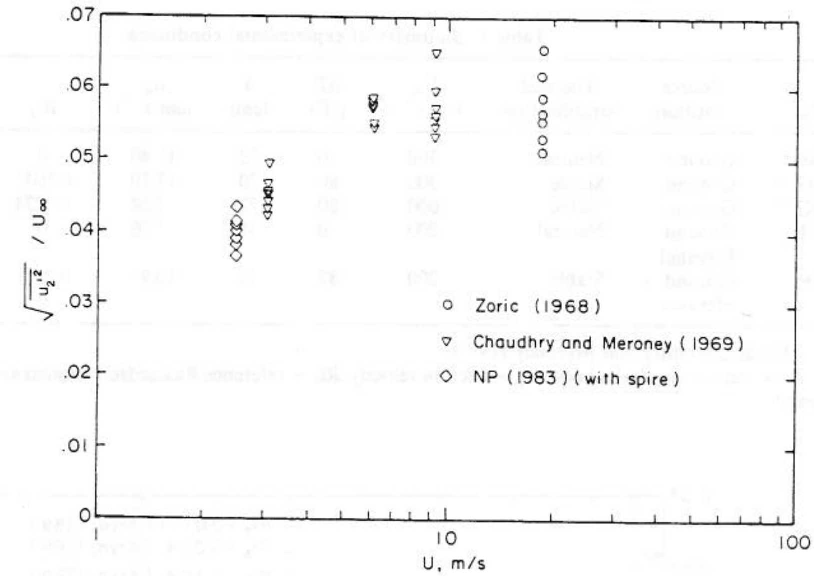

Fig. 3. Lateral turbulence intensity in neutrally stratified flow.

3.3. *Analysis of diffusion data*

The diffusion data from all wind tunnel measurements were expressed in terms of the standard deviations of the horizontal concentration profile. The standard deviation of the concentration, σ_2, is defined as

$$\sigma_2^2 = \frac{\Sigma C_j x_{2j}^2}{\Sigma C_j}, \tag{10}$$

where C_j is the mean concentration at a sampler, x_{2j} is the lateral distance from the maximum centerline concentration in the lateral direction at the same height and j is a particular sampler on the array.

The diffusion time T is approximated by the advection time scale x_1/U, where x_1 is the downwind distance from the source and U is the average mean velocity between source height and the sampler height.

4. PLUME DISPERSION DATA

Draxler summarized data from eleven field experiments for lateral and vertical diffusion downwind of surface and elevated releases under stable and unstable stratifications. Wind tunnel measurements are compared with these field measurements for horizontal diffusion from a ground source in Fig. 4. Only the data set for strong stable stratification ($Ri_\delta = 0.25$) deviate significantly from the field results. The lateral diffusion from an elevated source are plotted in Fig. 5 for comparison. The stable elevated case seems to deviate only slightly from the field experiments.

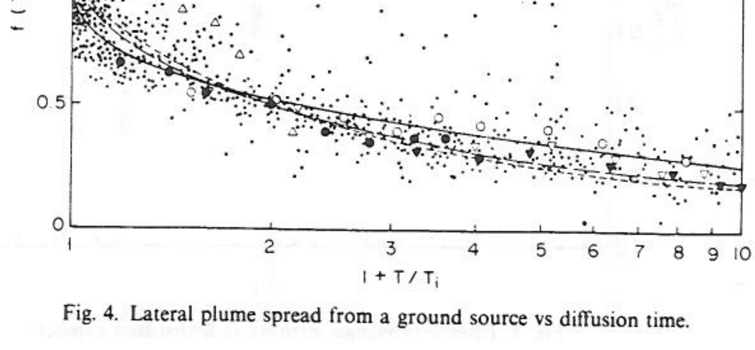

Fig. 4. Lateral plume spread from a ground source vs diffusion time.

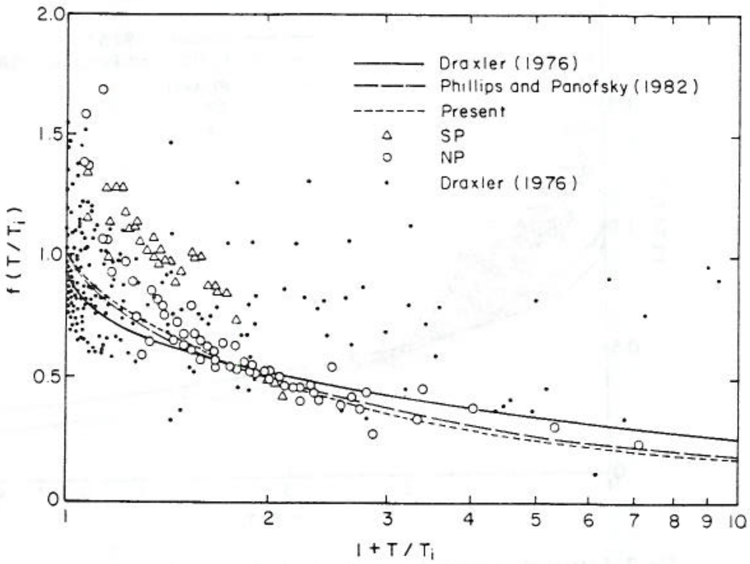

Fig. 5. Lateral plume spread from an elevated source vs diffusion time.

The stable elevated case has been considered separately so that a cleaner comparison with Draxler's results may be made. Draxler utilized an average T_i for a specified stratification category which applied to all experimental sites under that category in his analysis. Unfortunately, this approach results in points which are consistently greater than 0.5 in Fig. 6. This suggests that the actual value of T_i may be 3–4 times the value recommended by Draxler for the stable elevated source releases. In this case a replot of the field data would lie between $1+T/T_i = 1$ and 2, which agrees with the laboratory results.

Figure 7 displays the lateral diffusion measured at the same height as an elevated source. Plume width variations found for the elevated case in Fig. 7 should theoretically be described most accurately by Taylor's theory. Yet no significant improvement was found in comparison to Figs 4, 5 and 6.

4.1. *Data comparison with predictions*

The proportion of variation explained by prediction (or regressive curve), which describes the coherence between data and formulae, was examined by an analysis of variance. The experimental data employed in the analysis consisted of field experiments in Fig. 8 and laboratory results, except a stable stratification case SP. The correlation coefficient R appears to be acceptable for all three equations as shown in Table 2. The residual, $f_1(T/T_i) - \hat{f}_1(T/T_i)$, is displayed in Fig. 9(a) for field measurements and in Fig. 9(b) for laboratory results, where $\hat{f}_1(T/T_i)$ is the predicted value. The residuals were compared to a normal

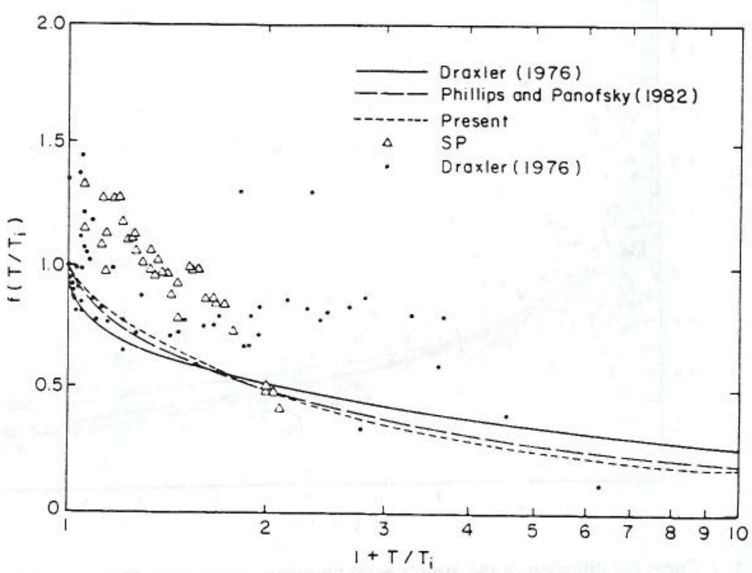

Fig. 6. Lateral plume spread in a stable stratified flow vs diffusion time.

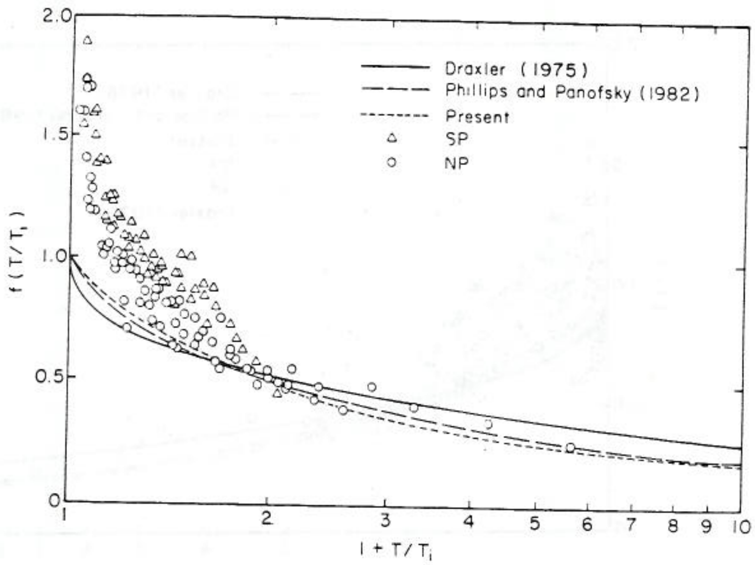

Fig. 7. Lateral plume spread at source height from an elevated source vs diffusion time.

$$\text{(I)}\quad \text{Curve 1:}\quad f(T/T_i) = \frac{1}{1 + 0.9\sqrt{T/T_i}}$$

$$\text{(II)}\quad \text{Curve 2:}\quad f(T/T_i) = 0.617\left[\frac{T_i}{T} - \frac{(T_i/T)^2}{5.25}\ln\left(1 + 5.25\frac{T}{T_i}\right)\right]^{1/2}$$

$$\text{(III)}\quad \text{Dash Curve:}\quad f(T/T_i) = 0.541\left[\frac{T_i}{T} - \frac{(T_i/T)^2}{6.83}\left(1 - \exp\left(-6.83\ T/T_i\right)\right)\right]^{1/2}$$

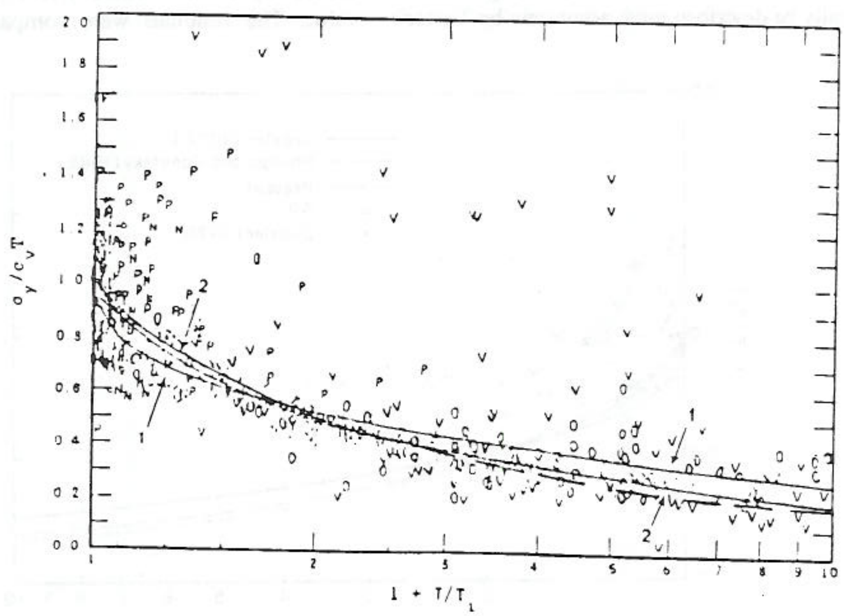

Fig. 8. f Curve for diffusion in the atmospheric boundary layer (from Phillips and Panofsky, 1982).

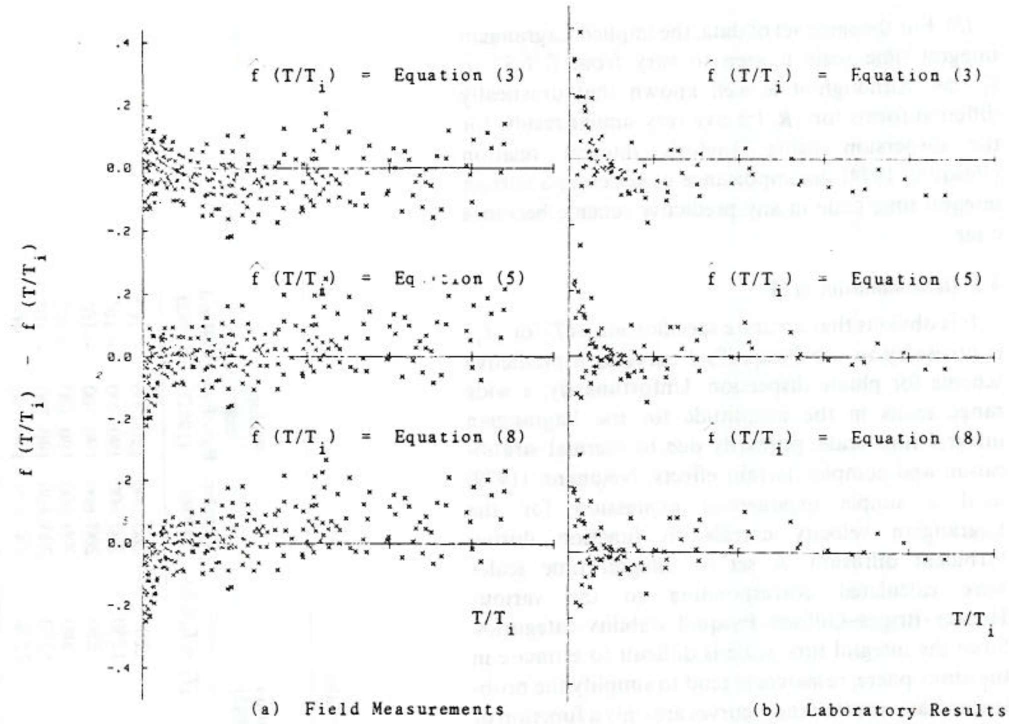

Fig. 9. Residual analysis for predictive schemes.

distribution by the Kolmogorov–Smirnov goodness of fit test (Conover, 1971). The level of significance in the test suggests that a normal distribution hypothesis is rejected by residuals of Equation (3). Therefore the probability distribution of residuals is presented in Table 2 together with the correlation coefficients. Equations (5) and (8) were found to fit the data slightly better. Yet no significant systematic deviation can be found among the three predictions during comparison with field or laboratory experimental results.

4.2. *Comparison among predictions*

Equations (3), (5) and (8) are plotted in Figs 5–8. Comparison between the predictive formulae and the experimental data reveals that:

(1) Difference among the three functional values are not significant. All of the expressions fit the trend of atmospheric field data as shown in Fig. 8. However the equations imply different values for the Lagrangian integral time scale, i.e. $T_i = 1.64\ {}_2T_L$ for (3), $T_i = 5.25\ {}_2T_L$ for (5) and $T_i = 6.83\ {}_2T_L$ for (8).

(2) The Lagrangian autocorrelation function corresponding to (5) preserves an exponential form for short diffusion times such that

$$ {}_2R_L(\tau) = e^{-2\tau/{}_2T_L} = \frac{1}{\left(1 + \frac{\tau}{{}_2T_L} + \dots\right)^2} \approx \frac{1}{(1 + \tau/{}_2T_L)^2}. \tag{9} $$

Neglecting higher order terms in the expressions prevents $f_1(T/T_i)$ from dropping rapidly at longer diffusion times. Since a higher correlation at larger times implies a larger value of the Lagrangian integral time scale, removal of higher order terms in the expansion results in an increase in the Lagrangian integral time scale for the same T_i; thus ${}_2T_L$ calculated from (5) is 1.3 times the value calculated from (8).

Table 2. Summary of comparison between data and predictions

	% of variation explained by the formula		Correlation coefficient R		Level of significance α†		Probability distribution of residual					
							$P(\lvert e\rvert \leq 0.05)$		$P(0.05 < \lvert e\rvert \leq 0.1)$		$P(\lvert e\rvert \geq 0.1)$	
Formula	Field exp.	Lab.* data	Field exp.	Lab. data	Field exp.	Lab. data	Field exp	Lab. data	Field exp.	Lab. data	Field exp.	Lab. data
Equation (3)	80.8	74.7	0.899	0.864	<0.01	<0.01	0.458	0.472	0.325	0.303	0.217	0.225
Equation (5)	78.9	84.5	0.888	0.919	0.09	0.03	0.496	0.618	0.292	0.225	0.212	0.157
Equation (8)	72.9	86.5	0.853	0.930	0.10	0.10	0.496	0.630	0.275	0.202	0.222	0.168

* Stable Stratification case SP is not included.

† Residuals were tested to a normal distribution function by the Kolmogorov–Smirnov goodness-of-fit test.

(3) For the same set of data, the implied Lagrangian integral time scale is seen to vary from $T_i/6.83$ to $T_i/1.64$. Although it is well known that drastically different forms for ${}_2R_L(\tau)$ give very similar results for the dispersion using Taylor's integral relation (Pasquill, 1974) the importance of selecting a correct integral time scale in any predictive scheme becomes clear.

4.3 *Determination of* T_i

It is obvious that accurate specification of T_i (or ${}_2T_L$) is necessary to use Pasquill's f curve as a predictive scheme for plume dispersion. Unfortunately, a wide range exists in the magnitude for the Lagrangian integral time scale, primarily due to thermal stratification and complex terrain effects. Neumann (1979) used a simple exponential expression for the Lagrangian velocity correlation function during turbulent diffusion. A set of integral time scales were calculated corresponding to the various Hosker–Briggs–Gifford–Pasquill stability categories. Since the integral time scale is difficult to estimate in the atmosphere, researchers tend to simplify the problem and assume that the f curves are only a function of downwind distance. Briggs (1973) suggested a dimensionally inconsistent function for the standard deviation of plume width. Hanna (1984) recommended a simplified function for the f curve compatible with Briggs' formula. Table 3 summarizes the integral time scale used (or implied) by the different authors. The variation is indeed astonishing. ${}_2T_L$ varies from several hundred seconds as predicted by Draxler (1976) to an order of 10^4 s as suggested by Gifford (1982). All these time scales are based on field measurements in the atmosphere, although their stability classification and the flow configuration may vary. Hence additional knowledge about the integral time scale and how it relates to basic physical characteristics of a turbulent shear layer is required.

T_i may be used to specify the Lagrangian integral time scale ${}_2T_L$, since the Lagrangian autocorrelation function is implied in the f curve relationship in (5) and (8). If r stands for the ratio of T_i/T and one assumes that $f(1) = b$, $0 < b < 1$, then r can be evaluated once b is defined. Algebraic manipulation indicates that $b^2 = 2[(1/r) - (1/r^2)(1 - e^{-r})]$ and $b^2 = 2[(1/r) - (1/r^2)\ln(1 + r)]$ for (5) and (8), respectively. If the turbulence is stationary and homogeneous, T_i must be constant regardless of which value of b is chosen.

Draxler (1976) found that for some conditions a larger T_i seems to be indicated at large travel times. He suspected that wind shear causes additional lateral diffusion, which is not taken into account by the simple theory. To compensate for wind shear effects he suggested a simple algorithm which fits Taylor's limit for large T. Of course varying T_i results in various ${}_2T_L$ values. This may be realistic if turbulent characteristics vary over a complex terrain topology. On the other hand different ${}_2T_L$ may also be obtained at large T by setting b to an asymptotic value such as $b = 0.2$.

Table 3. Summary of Lagrangian integral time scales

Stability category	$\overline{u_2'^2}$ $(\mathrm{m\,s^{-1}})^2$	u $\mathrm{m\,s^{-1}}$	${}_2T_L$ (s) Neumann (1978)	Briggs (1973) ${}_2T_L = T_i/5.23$	Briggs (1973) ${}_2T_L = T_i/6.83$	Hanna (1982) ${}_2T_L = T_i/5.23$	Hanna (1982) ${}_2T_L = T_i/6.83$	Draxler (1976)	Phillips and Panofsky (1982)	Gifford (1982)
A	0.19	2	2400	2900	2200	2900	2200	200–600	190–700	~ 10^4
B	0.24	3.5	1700	2300	1800	1640	1250	200–600	190–700	~ 10^4
C	0.36	5	700	900	690	1050	880	200–600	190–700	~ 10^4
D	0.17	5	750	1070	820	1030	880	200–600	190–700	~ 10^4
E	0.044	3.5	1000	1640	1250	1640	1250	200–600	190–700	~ 10^4
F	0.0064	2	2250	2900	2200	2900	2200	200–600	190–700	~ 10^4

4.4. *An alternative method*

The atmospheric boundary layer wind tunnel reproduces comparable data to the field experiments even without detailed simulation of terrain properties and turbulent statistics. With the help of boundary augmentation devices and turbulent flow control facilities, the wind tunnel also replicates plume behavior in the atmospheric boundary layer.

Several sets of Eulerian space–time correlation data from laboratory experiments are collected in Fig. 9 to compare with the present correlation measurements. These experiments include data measured in grid turbulence corrected for energy decay (Comte-Bellot and Corrsin, 1971) and data in nearly homogeneous turbulent shear flow (Harris *et al.*, 1977). A universal functional form of the Eulerian space-time correlation seems to exist in Fig. 10. Table 4 includes the integral time scale of Eulerian space–time correlation, T_s, estimated from the correlation measurements to compare with ${}_2T_L$ estimated from diffusion measurements.

Experiments which include simultaneously both velocity correlation measurements and diffusion measurements are rare. An exception for the grid turbulence case was reported by Schlein and Corrsin (1974). They performed measurements of thermal diffusion downstream of a heated wire in the same facility which had previously been very thoroughly mapped for Eulerian turbulence properties by Comte-Bellot and Corrsin. They inferred a Lagrangian autocorrelation function by employing the second derivative of the measured lateral wake spread. (Differentiating experimental data twice introduces a large likelihood of error.) The value was slightly larger than the measured Eulerian space–time correlation, at least in the range $0.25 < {}_2R_L(\tau) < 1.0$. Shlein and Corrsin reported that ${}_2T_L/T_s = 1.3$ in a turbulence field which is normalized to the conditions existing at $Ut/M = 42$, where M is the mesh size. Their results agree with present experimental results in the lower part of boundary layer as seen in Table 3.

Laboratory measurements thus suggest a more

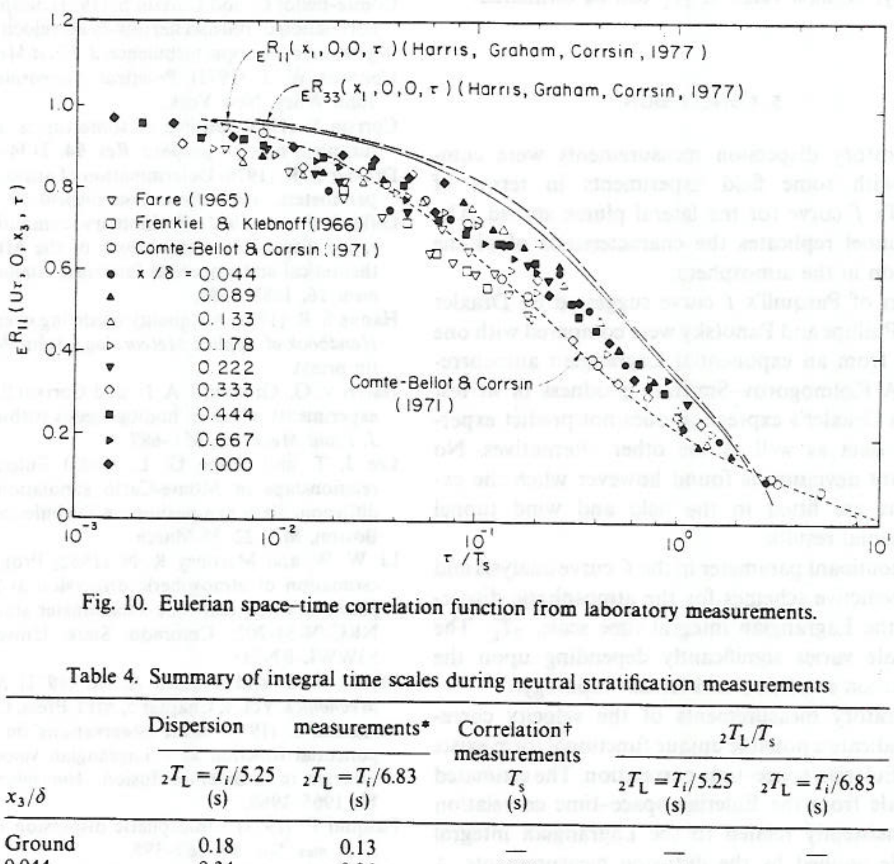

Fig. 10. Eulerian space–time correlation function from laboratory measurements.

Table 4. Summary of integral time scales during neutral stratification measurements

	Dispersion measurements*		Correlation† measurements	${}_2T_L/T_s$	
x_3/δ	${}_2T_L = T_i/5.25$ (s)	${}_2T_L = T_i/6.83$ (s)	T_s (s)	${}_2T_L = T_i/5.25$ (s)	${}_2T_L = T_i/6.83$ (s)
Ground	0.18	0.13			
0.044	0.34	0.26	0.23	1.48	1.13
0.189	0.63	0.48	0.44	1.43	1.09
0.133	0.68	0.52	0.51	1.33	1.02
0.178	0.78	0.60	0.65	1.20	0.92
0.222	0.80	0.62	0.70	1.14	0.88
0.333	0.83	0.64	0.91	0.91	0.70
0.444	0.85	0.65	1.00	0.85	0.65

* Dispersion data was taken at the same height as an elevated source.
† Turb fluctuations below 2 Hz were removed with a high pass filter.

accurate way to estimate the Lagrangian integral time scale for application in predictive schemes for plume dispersion. By utilizing a few anemometers in the field, basic turbulence characteristics such as $\overline{u_2'^2}$, U, T and T_E may be obtained, where T_E is the Eulerian time scale. Given a particular Eulerian space–time correlation and diffusion time from two separated anemometers, then T_s at that particular site during the real time meteorological conditions can be evaluated using the universal functional form displayed on Fig. 9. Baldwin and Johnson (1975) proposed a simple scheme of numerical iteration to estimate the Lagrangian time scale from the Eulerian space–time correlation and Corrsin's independence hypothesis. Lee and Stone (1983) adopted the idea in their Monte-Carlo simulation of Langevin equation in atmospheric dispersion (Corrsin, 1959). They have attained quite successful results which are compatible with theoretical prediction. In turn, either from the resemblence of the Lagrangian time scale to the Eulerian space–time integral scale, or from the Baldwin and Johnson's approach (Li and Meroney, 1982), a value of ${}_2T_L$ can be estimated.

5. CONCLUSION

Laboratory dispersion measurements were compared with some field experiments in terms of Pasquill's f curve for the lateral plume spread. The wind tunnel replicates the characteristics of plume dispersion in the atmosphere.

Forms of Pasquill's f curve suggested by Draxler and by Phillips and Panofsky were compared with one derived from an exponential Lagrangian autocorrelation. A Kolmogorov–Smirnov goodness of fit test suggests Draxler's expression does not predict experimental data as well as the other alternatives. No significant deviation is found however when the expressions are fitted to the field and wind tunnel experimental results.

The dominant parameter in the f curve analysis and most predictive schemes for the atmospheric dispersion is the Lagrangian integral time scale, ${}_2T_L$. The time scale varies significantly depending upon the stratification condition and terrain topology.

Laboratory measurements of the velocity correlation indicate a possible unique functional form exists for the Eulerian space–time correlation. The estimated time scale from the Eulerian space–time correlation was consistently related to the Lagrangian integral time sale implied by the diffusion measurements. A more accurate estimation of ${}_2T_L$ in the atmosphere through laboratory verification provides better prediction of the plume spread.

Acknowledgements—Discussions with Dr. H. A. Panofsky and Dr. R. F. Abbey (NRC) are acknowledged. Statistical support by Dr. M. M. Siddiqui and Ms C. C. Wang is appreciated. Financial support from Nuclear Regulatory Commission, Project NRC-04-81-202, made this study possible. Comments and suggestions received from the referees are appreciated.

REFERENCES

Arya S. P. S. (1968) Structure of stably stratified turbulent boundary layer. Ph.D. dissertation, Colorado State University, CER68-69SPSA10.

Balwin L. V. and Johnson G. R. (1972) The estimation of turbulent diffusivities from anemometer measurements—I. Fluid particles. Colorado State University, CEP71-72LVB-GRJ42.

Briggs G. A. (1973) Diffusion estimation for small emissions. Air Resources Atmospheric Turbulence and Diffusion Laboratory, USAEC Report ATDL-106, NOAA.

Cermak J. E. (1982) Physical modeling of the atmospheric boundary layer in long boundary-layer wind tunnel. In *Wind Tunnel Modeling for Civil Engineering Applications* (Edited by Reinhold T. A.), pp. 97–125. Cambridge University Press Cambridge.

Chaudhry F. H. and Meroney R. N. (1973) A laboratory study of diffusion in stable stratified flow. *Atmospheric Environment* **7**, 443–454.

Comte-Bellot G. and Corrsin S. (1971) Simple Eulerian time correlation of full and narrow-band velocity signals in grid-generated isotropic turbulence. *J. Fluid Mech.* **48**, 273–337.

Conover W. J. (1971) *Practical Nonparametric Statistics.* John Wiley, New York.

Corrsin S. (1959) Outline of some topics in homogeneous turbulent flow. *J. geophys. Res.* **64**, 2134–2150.

Draxler R. R. (1976) Determination of atmospheric diffusion parameters. *Atmospheric Environment* **10**, 99–105.

Gifford F. A. (1982) Preliminary communication.: Long range dispersion: comparisons of the Mt. Isa data with theoretical and emperical formulas. *Atmospheric Environment* **16**, 1583–1586.

Hanna S. R. (1984) Air quality modeling over short distance. *Handbook of Applied Meteorology*. John Wiley, New York (in press).

Harris V. G., Graham J. A. H. and Corrsin S. (1977) Further experiments in nearly homogeneous turbulent shear flow. *J. Fluid Mech.* **81**, 651–687.

Lee J. T. and Stone G. L. (1983) Eulerian–Lagrangian relationships in Monte-Carlo simulations of turbulent diffusion. Sixth Symposium on Turbulence and Diffusion, Boston, MA, 22–25 March.

Li W. W. and Meroney R. N. (1982) Progress report: the estimation of atmospheric dispersion at nuclear reactor plants utilizing real time anemometer statistics. Contract NRC-04-81-202, Colorado State University, CER82-83WWL-RNM1.

Monin A. S. and Yaglom A. M. (1971) *Statistical Fluid Mechanics*. Vol. 1, Chapter 5, MIT Press, Cambridge, MA.

Neumann J. (1978) Some observations on the simple exponential function as a Lagrangian velocity correlation function in turbulent diffusion. *Atmospheric Environment* **12**, 1965–1968.

Pasquill F. (1971) Atmospheric dispersion of pollution. *Q. Jl R. met. Soc.* **97**, 369–395.

Pasquill F. (1974) *Atmospheric Diffusion*. Chapter 3, Section 3.5, Halsted Press.

Phillips P. and Panofsky H. A. (1982) A re-examination of lateral dispersion from continuous sources. *Atmospheric Environment* **16**, 1851–1859.

Plate E. J. and Cermak J. E. (1963) Micrometeorological wind tunnel tunnel facility, description and characteristics. Colorado State University, CER63EJP-JEC9.

Shlein D. J. and Corrsin S. (1974) A measurements of Lagrangian velocity auto-correlation in approximately isotropic turbulence. *J. Fluid Mech.* **62**, 255–271.

Taylor G. I. (1921) Diffusion by continuous moment. *Proc. R. Math. Soc.* **A20**, 196–211.

Tennekes H. (1979) The exponential Lagrangian correlation function and turbulent diffusion in the inertial subrange. *Atmospheric Environment* **13**, 1565–1567.

Zoric D. L. (1968) Approach of turbulent boundary layer to similarity. Technical Report, Colorado State University, Grant DA-AMC-28-043-65-G20, CER68-69DLZ9.